Observation of Parametric Instability in Advanced LIGO

Matthew Evans,* Slawek Gras, Peter Fritschel, John Miller, and Lisa Barsotti
Massachusetts Institute of Technology, Cambridge, Massachusetts 02139, USA

Denis Martynov, Aidan Brooks, Dennis Coyne, Rich Abbott, Rana X. Adhikari, Koji Arai, Rolf Bork, Bill Kells, Jameson Rollins, Nicolas Smith-Lefebvre, Gabriele Vajente, and Hiroaki Yamamoto
California Institute of Technology, Pasadena, California 91125, USA

Carl Adams, Stuart Aston, Joseph Betzweiser, Valera Frolov, Adam Mullavey, Arnaud Pele, Janeen Romie, Michael Thomas, and Keith Thorne
LIGO Livingston Observatory, Livingston, Louisiana 70754, USA

Sheila Dwyer, Kiwamu Izumi, Keita Kawabe, and Daniel Sigg
LIGO Hanford Observatory, Richland, Washington 99352, USA

Ryan Derosa, Anamaria Effler, and Keiko Kokeyama
Louisiana State University, Baton Rouge, Louisiana 70803, USA

Stefan Ballmer and Thomas J. Massinger
Syracuse University, Syracuse, New York 13244, USA

Alexa Staley
Columbia University, New York, New York 10027, USA

Matthew Heinze and Chris Mueller
University of Florida, Gainesville, Florida 32611, USA

Hartmut Grote
Max Planck Institute for Gravitational Physics, 30167 Hannover, Germany

Robert Ward
Australian National University, Canberra, Australian Capital Territory 0200, Australia

Eleanor King
University of Adelaide, Adelaide, South Australia 5005, Australia

David Blair, Li Ju, and Chunnong Zhao
University of Western Australia, Crawley Western Australia 6009, Australia

(Received 7 March 2015; published 23 April 2015)

Parametric instabilities have long been studied as a potentially limiting effect in high-power interferometric gravitational wave detectors. Until now, however, these instabilities have never been observed in a kilometer-scale interferometer. In this Letter, we describe the first observation of parametric instability in a gravitational wave detector, and the means by which it has been removed as a barrier to progress.

DOI: 10.1103/PhysRevLett.114.161102 PACS numbers: 04.80.Nn, 42.50.Wk, 42.79.Jq, 95.55.Ym

Introduction.—Optomechanical interactions, the moving of masses by radiation pressure, are typically of such a tenuous nature that even carefully designed experiments may fail to observe them. In the extreme environment of a high-power interferometric gravitational wave detector, however, these effects arise spontaneously. This is true despite the fact that these instruments feature multikilogram optics [1], unlike the microgram or nanogram optics generally used in experiments which target such effects [2–5].

Hence, gravitational wave detectors provide an extraordinary platform from which to explore the optomechanical couplings which give rise to optical springs, optical cooling, ponderomotive squeezing, and quantum-mechanical entanglement, all with undeniably macroscopic objects [1,6–9]. These opportunities are not without cost; the

radiation pressure associated with high circulating power can destabilize interferometer alignment [10] and lead to parametric instabilities.

Since the seminal work of Braginsky *et al.* in 2001 [11], optical parametric instabilities have been extensively studied as a potential limit to high-power operation of interferometric gravitational wave detectors [12–41].

We report on the first observation of a self-sustaining parametric instability in a gravitational wave detector and the subsequent quenching of this instability. This observation, at the Laser Interferometer Gravitational Wave Observatory (LIGO) Livingston Observatory (LLO) [42], is the culmination of more than a decade of theoretical calculation, numerical modeling, and laboratory-scale experimentation. Although reasonable agreement between theoretical prediction and observed parametric instabilities has been documented previously in dedicated experiments using MHz oscillators [14,41], this observation serves as confirmation that models which have been built to understand the phenomenon in the complex setting of a gravitational wave interferometer are substantially correct.

A wide variety of techniques have been suggested for overcoming parametric instabilities in gravitational wave detectors [43–49], most of which fall into a few notable categories: avoid instability by changing the radius of curvature of one or more optics [43,49], actively damp mechanical modes as they become excited [48], and prevent instability by increasing the loss of the test mass mechanical modes with passive dampers [35,45,46,50]. The first of these techniques has been demonstrated and found to be effective at LLO.

Theory of Parametric Instability.—Parametric instabilities (PI) operate by transferring energy from the fundamental optical mode of the interferometer, which with nearly 1 MW of circulating power can be as much as 40 J, into an interferometer optic's mechanical mode (see Fig. 1). Energy transfer takes place via the radiation pressure driven optomechanical interaction and the modulation of the fundamental field by the excited mechanical mode [31] (see Fig. 1).

The parametric gain for a given test mass mechanical mode is given by

$$R_m = \frac{8\pi Q_m P_{\mathrm{arm}}}{M\omega_m^2 c\lambda} \sum_{n=0}^{\infty} \mathrm{Re}[G_n] B_{m,n}^2 \qquad (1)$$

(using the notation of Ref. [31], and correcting an error therein [51]). The fixed parameters used in Eq. (1) are: c the speed of light, λ the laser wavelength, M the mass of the optic, ω_m the angular resonant frequency of mechanical mode with index m, and $B_{m,n}$ the overlap between mechanical mode m and optical mode n. Parameters subject to manipulation are, the power stored in the interferometer arm cavities P_{arm}, the quality factor of a given mechanical mode Q_m, and the optical gain of the optical mode G_n, of which $\mathrm{Re}[G_n]$ is the real part.

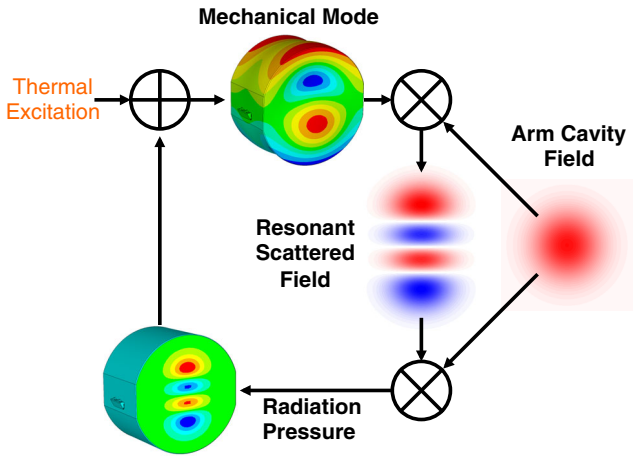

FIG. 1 (color online). Parametric instabilities transfer energy from the arm cavity field to a mechanical mode of an interferometer test mass. Since the rate of energy transfer depends on the amplitude of the excited mechanical mode, this can be a runaway positive feedback process.

Clearly, the potential for instability grows with increasing power, since the parametric gain of all modes is proportional to P_{arm}. Active and passive damping techniques for defusing PI operate by reducing the Q of an otherwise unstable mechanical mode, while avoidance techniques work by changing the optical gain G_n to prevent instability.

The e-fold growth time for an unstable mode is given by

$$\tau_m = \frac{2Q_m}{\omega_m(R_m - 1)}. \qquad (2)$$

Note that for $R_m = 0$, this gives a negative value equal to the usual decay time of a mechanical mode with frequency $f_m = \omega_m/2\pi$ and quality factor Q_m. For values of $R_m > 1$, Eq. (2) gives a positive value, indicating exponential growth.

The circulating power level P_{arm} at which a mode becomes unstable is referred to as the threshold power $\bar{P}_m$ for that mode and is found by rearranging Eq. (1) with $R_m = 1$ and $P_{\mathrm{arm}} = \bar{P}_m$. At threshold, the optomechanical interaction is putting energy into the mode at the same rate that it is being dissipated, so $\tau_m \to \infty$.

Observed Parametric Instability.—Parametric instability was first observed in the Advanced LIGO detector recently installed at LLO (see Ref. [52] for detailed information about the detectors). The instability grew until it polluted the primary gravitational wave output of the detector by aliasing into the detection band and saturating detection electronics (see Fig. 2). The time scale for growth was long enough to allow for manual intervention (a reduction of the

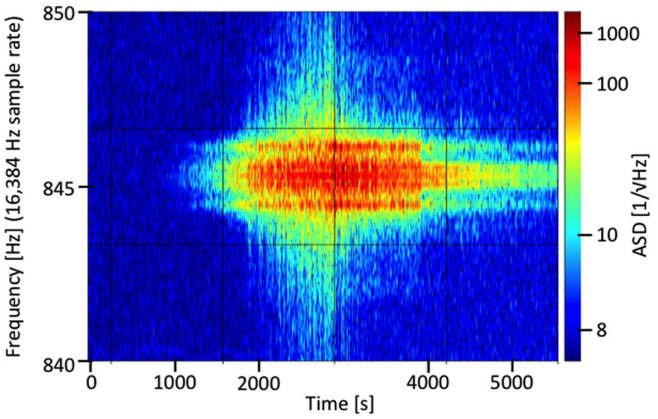

FIG. 2 (color online). The excitation due to parametric instability was first observed as an exponentially growing feature in the detector's primary output (the gravitational wave channel). The feature is aliased into the detector band by the 16384 Hz sample rate of the digital system which causes it to appear at 845 Hz. The growing instability eventually causes saturation of the electronic readout chain, which appears as broadband contamination of the detector output channel (visible between 2500 and 3000 s). In the above data, the power into the interferometer was decreased before saturation caused the interferometer control systems to fail (see Fig. 4).

laser power input to the interferometer) before control was lost due to this saturation of the readout electronics.

The test mass (TM) mechanical mode responsible for the instability was identified as the 15.54 kHz mode shown in Fig. 3. The higher-order mode spacing of the Advanced LIGO arm cavities is 5.1 ± 0.3 kHz, and the optical resonance width is 80 Hz, such that a 3rd order transverse optical mode can provide energy transfer from the fundamental optical mode to this mechanical mode (see Figs. 1 and 3).

By measuring the e-folding growth and decay time of the excited acoustic mode as a function of circulating power in the interferometer arm cavities, we can compute the parametric gain R and mechanical mode quality factor Q as given in Eq. (2). Our measurements were performed by operating the interferometer above the threshold power to excite the TM mechanical mode and then reducing the power below the instability threshold and watching the mode amplitude decrease, as shown in Fig. 4.

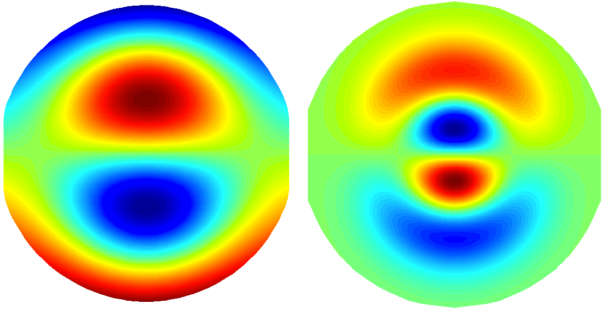

FIG. 3 (color online). The test mass mechanical mode and cavity optical mode responsible for the observed parametric instability are shown. The left panel is the test mass front surface displacement due to the mechanical mode, while the right panel is the radiation pressure induced displacement (red is positive and blue negative in both panels). Both of these modes occur at 15.5 kHz and they have an overlap factor of $B_{m,n} = 0.1$.

The observed unstable mode has $R = 2$ with $P_{\mathrm{arm}} = 50$ kW, and the associated mechanical mode has $Q = 12 \times 10^6$. This Q factor is in the range expected given similar measurements of Advanced LIGO test masses [48,53], and the parametric gain is as predicted by Eq. (1) for a high, but far from maximal value of G_n. While the 90% confidence limit for this mode is $R = 11$, as seen in Fig. 5, 5% of simulated values are higher than the observed value, and 1% have $R > 100$.

Defusing Parametric Instability.—Parametric instability depends on several potentially modifiable features of a gravitational wave detector, two of which can be exploited in Advanced LIGO without modifying the interferometer core optics.

First, instability requires that a test mass mechanical mode and an arm cavity optical mode have coincident resonant frequencies [i.e., G_n in Eq. (1) must be large at the mechanical mode frequency ω_m for an optical mode with nonvanishing overlap $B_{m,n}$]. Through its effect on transverse mode spacing, changing the radius of curvature (ROC) of one of the test masses in the cavity affected by PI can remove any coincidence. Advanced LIGO arm

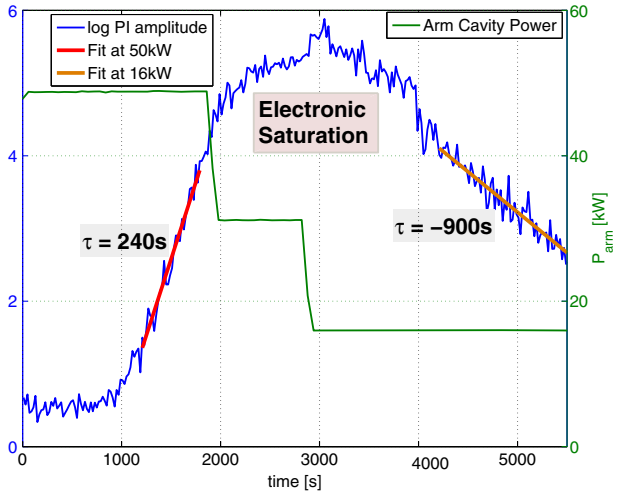

FIG. 4 (color online). The amplitude of the excitation shown in Fig. 2 is fitted at times with different values of P_{arm} to find its growth (or decay) time scale as a function of power. The growth of the PI is clearly visible above the noise after 1000 s, with an e-folding growth time of 240 s, until 2000 s at which point the readout electronics begin to saturate. A little more than 4000 s into the plotted data, the excited mechanical mode is seen decaying with $\tau = -900$ s. According to Eq. (2), these data imply a threshold power of 25 kW and $Q = 12 \times 10^6$ for this mode.

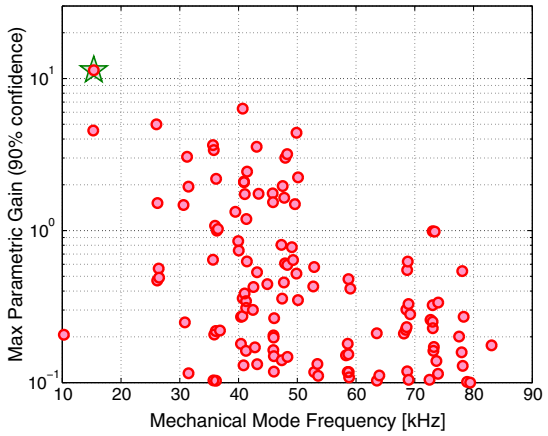

FIG. 5 (color online). The maximum gain expected at full power, $P_{\mathrm{arm}} = 800$ kW, for all potentially unstable modes (90% confidence value for a single test mass). Since the mechanical mode frequencies and optics parameters are known with limited precision, the parametric gain of a particular mode cannot be computed exactly, and Monte Carlo methods must be used [31]. The "90% confidence maximum" shown here is the value for which 90% of the 342 881 Monte Carlo computations gave a lower gain. Notably, the observed unstable mode is the mode with the highest predicted parametric gain (marked with a green star), and the observed gain is about a factor of 3 higher than the value shown here ($R = 2$ at 50 kW, or $R = 32$ at 800 kW). This is not so much bad luck as a trials factor; there are four test masses and many potentially unstable modes, and the statistics shown in Fig. 7 confirm quantitatively that the observation of at least one unstable mode was to be expected.

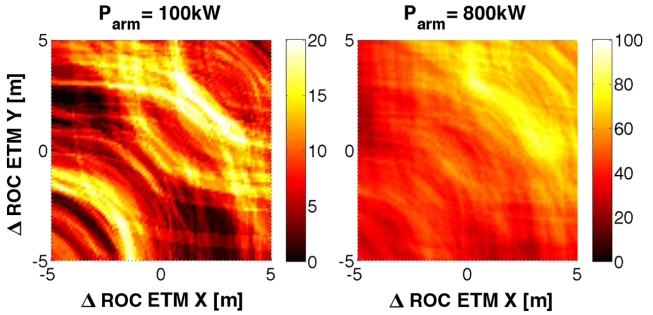

FIG. 6 (color online). The number of unstable modes as a function of change in arm cavity mirror radius of curvature (ROC), as indicated by the color scale to the right of each plot. With 100 kW of circulating power, as expected for the first observing run, small changes in mirror ROC can be used to avoid parametric instability. Higher power levels, however, increase parametric gain; note the different color scales used on the left and right panels. At Advanced LIGO's design operating power of $P_{\mathrm{arm}} = 800$ kW, ROC adjustments can at best be used to reduce the number of unstable modes.

cavities use mirrors with ~2 km ROC, so for the 3rd order optical mode shown in Fig. 3, for example, a change of 1 m is sufficient to change its resonant frequency by 80 Hz, or one cavity linewidth.

Shortly after the first PI was observed at LLO, heating elements, known as "ring heaters", were used to change the mirror ROC and avoid the instability. Ring heaters were included in the Advanced LIGO design to compensate for ROC changes due to absorption of the fundamental optical mode, and can change the ROC of the optics by several tens of meters. After adjusting the ring heaters to produce roughly 2 m of ROC change of the arm-cavity end mirrors, the parametric gain of the observed instability at 15.53 kHz was reduced below unity, and the interferometer was operated with nearly 100 kW of circulating power for more than 12 h.

Despite this success, it must be recognized that many mechanical modes of the interferometer test masses can be driven to instability; Fig. 5 shows the maximum expected parametric gain of all potentially unstable modes. From the left panel of Fig. 6, we can conclude that using the ring heaters to find a PI-free zone is likely to succeed at present (with $P_{\mathrm{arm}} \sim 100$ kW), but the right panel tells us that at the design value of $P_{\mathrm{arm}} = 800$ kW ROC changes alone will not be sufficient.

Alternatively, instability can be avoided by increasing the energy loss (decreasing the Q) of the mechanical modes of the test mass through active or passive damping. As can be inferred from the linear dependence of R_m on Q_m in Eq. (1), the weak radiation pressure coupling of energy from the fundamental optical mode to the mechanical modes of the test mass must be sufficient to overcome the energy loss of the mechanical mode in order for instability to be reached. The quality factor of mechanical modes in the Advanced LIGO test mass optics is roughly 10^7, and as such, is easily spoiled. Since the highest parametric gain likely to be seen in Advanced LIGO is ~10, reducing Q_m to less than 10^6 for potentially unstable modes would suffice (see Fig. 5).

In anticipation of PI, all Advanced LIGO test masses were outfitted with electrostatic actuators capable of damping mechanical modes (including the observed mode) associated with PI [48]. This method of damping TM mechanical modes has been demonstrated at MIT with a prototype Advanced LIGO optic, but has not yet been tested at LLO since the required feedback loop has not been implemented, and ROC changes were immediately available and decisively effective.

Several major periods of data taking are expected with Advanced LIGO at power levels below the design power [54]. Figure 7 shows the number of modes that are likely to be unstable as a function of circulating power in the interferometer.

If a manageable number of unstable modes is encountered, the combination of the above techniques will likely prove adequate, with ROC changes reducing the number of unstable modes and electrostatic actuators actively damping the remaining instabilities. If, however, the number of unstable modes becomes so large (at the final operating

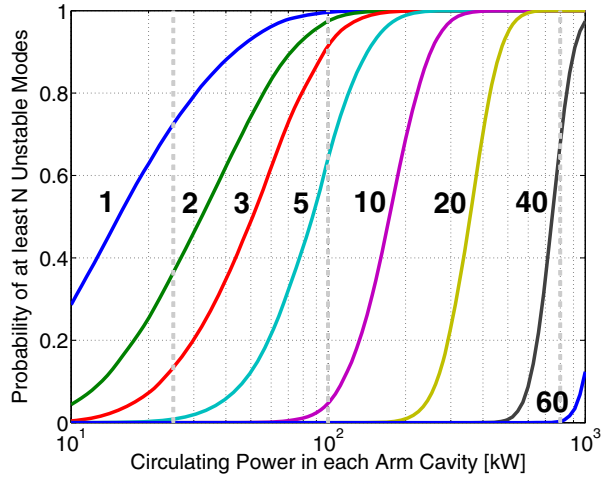

FIG. 7 (color online). The probabilities of having various numbers of unstable modes anywhere in the interferometer (with four test masses), as a function of circulating power, P_{arm}. Each curve gives the probability that at least $N = \{1, 2, 3, 5, \ldots\}$ unstable modes are observed in an Advanced LIGO interferometer at a given level of circulating power in the arm cavities. The vertical gray lines mark the threshold power of the mode first observed to be unstable, near 25 kW of circulating power, the power level at which the first observing run of Advanced LIGO is planned, roughly 100 kW, and the design power level of 800 kW. These data indicate that more than 40 modes will likely need to be damped or otherwise defused in order to operate at 800 kW.

power, for instance, more than 40 modes are likely to be unstable) that the use of the electrostatic drives requires unreasonable human commissioning time or that the drive itself begins to saturate, a passive approach may be preferable. A broadband test mass Q reduction, which simultaneously targets many potentially unstable modes, may be achieved by mounting small piezoelectric dampers on the test masses [53].

Conclusions.—Parametric instabilities, studied in great depth and feared as a limitation to the attainable operating powers of interferometric gravitational wave detectors, have been observed for the first time in an Advanced LIGO detector. The behavior of the observed instability was found to be largely in agreement with models of the effect, implying that no significant ingredients have been omitted in the theoretical analysis.

Furthermore, the observed PI has been quenched by thermally tuning the optical resonance of the interferometer away from the resonance of the associated mechanical mode. This approach to PI, while sufficient for a small number of potentially unstable modes, may not be sufficient at higher operating powers where many modes are available for runaway excitation.

Thanks to many years of theoretical and experimental work on parametric instabilities, now informed by the observations described in this Letter, the challenge faced by high-power interferometric gravitational wave detectors is clear and well understood. While the necessary mitigation techniques are not trivial, a suitable combination of thermal tuning, active damping of excited mechanical modes, and passive reduction of mechanical mode Q factors is expected to be sufficient to allow Advanced LIGO to operate stably at full power.

The authors would like to acknowledge the extensive theoretical analysis of parametric instabilities by our Moscow State University colleagues Vladimir Braginsky, Sergey Strigin, and Sergey Vyatchanin, without which these instabilities would have come as a terrible surprise. LIGO was constructed by the California Institute of Technology and Massachusetts Institute of Technology with funding from the National Science Foundation, and operates under Cooperative Agreement No. PHY-0757058. Advanced LIGO was built under Grant No. PHY-0823459.

*mevans@ligo.mit.edu

[1] LIGO Scientific Collaboration, New J. Phys. **11**, 073032 (2009).
[2] T. J. Kippenberg and K. J. Vahala, Opt. Express **15**, 17172 (2007).
[3] T. J. Kippenberg and K. J. Vahala, Science **321**, 1172 (2008).
[4] D. McClelland, N. Mavalvala, Y. Chen, and R. Schnabel, Laser Photonics Rev. **5**, 677 (2011).
[5] M. Poot and H. S. J. van der Zant, Phys. Rep. **511**, 273 (2012).
[6] A. Buonanno and Y. Chen, Class. Quantum Grav. **19**, 1569 (2002).
[7] H. J. Kimble, Y. Levin, A. B. Matsko, K. S. Thorne, and S. P. Vyatchanin, Phys. Rev. D **65**, 022002 (2001).
[8] W. Marshall, C. Simon, R. Penrose, and D. Bouwmeester, Phys. Rev. Lett. **91**, 130401 (2003).
[9] H. Müller-Ebhardt, H. Rehbein, C. Li, Y. Mino, K. Somiya, R. Schnabel, K. Danzmann, and Y. Chen, Phys. Rev. A **80**, 043802 (2009).
[10] K. L. Dooley, L. Barsotti, R. X. Adhikari, M. Evans, T. T. Fricke, P. Fritschel, V. Frolov, K. Kawabe, and N. Smith-Lefebvre, J. Opt. Soc. Am. A **30**, 2618 (2013).
[11] V. B. Braginsky, S. E. Strigin, and S. P. Vyatchanin, Phys. Lett. A **287**, 331 (2001).
[12] V. B. Braginsky, S. E. Strigin, and S. P. Vyatchanin, Phys. Lett. A **305**, 111 (2002).
[13] S. W. Schediwy, C. Zhao, L. Ju, and D. G. Blair, Class. Quantum Grav. **21**, S1253 (2004).
[14] T. J. Kippenberg, H. Rokhsari, T. Carmon, A. Scherer, and K. J. Vahala, Phys. Rev. Lett. **95**, 033901 (2005).
[15] L. Ju, S. Grass, C. Zhao, J. Degallaix, and D. G. Blair, J. Phys. Conf. Ser. **32**, 282 (2006).
[16] L. Ju, S. Gras, C. Zhao, J. Degallaix, and D. G. Blair, Phys. Lett. A **354**, 360 (2006).
[17] L. Ju, C. Zhao, S. Gras, J. Degallaix, D. G. Blair, J. Munch, and D. H. Reitze, Phys. Lett. A **355**, 419 (2006).
[18] A. G. Gurkovsky, S. E. Strigin, and S. P. Vyatchanin, Phys. Lett. A **362**, 91 (2007).
[19] S. E. Strigin and S. P. Vyatchanin, Phys. Lett. A **365**, 10 (2007).

[20] I. A. Polyakov and S. P. Vyatchanin, Phys. Lett. A **368**, 423 (2007).
[21] A. G. Gurkovsky and S. P. Vyatchanin, Phys. Lett. A **370**, 177 (2007).
[22] S. W. Schediwy, C. Zhao, L. Ju, D. G. Blair, and P. Willems, Phys. Rev. A **77**, 013813 (2008).
[23] S. P. Vyatchanin and S. E. Strigin, IEEE J. Quantum Electron. **37**, 1097 (2007).
[24] C. Zhao, L. Ju, Y. Fan, S. Gras, B. J. J. Slagmolen, H. Miao, P. Barriga, D. G. Blair, D. J. Hosken, A. F. Brooks, P. J. Veitch, D. Mudge, and J. Munch, Phys. Rev. A **78**, 023807 (2008).
[25] S. E. Strigin, D. G. Blair, S. Gras, and S. P. Vyatchanin, Phys. Lett. A **372**, 5727 (2008).
[26] S. E. Strigin, Phys. Lett. A **372**, 6305 (2008).
[27] H. Miao, C. Zhao, L. Ju, S. Gras, P. Barriga, Z. Zhang, and D. G. Blair, Phys. Rev. A **78**, 063809 (2008).
[28] C. Zhao, L. Ju, H. Miao, S. Gras, Y. Fan, and D. G. Blair, Phys. Rev. Lett. **102**, 243902 (2009).
[29] V. V. Meleshko, S. E. Strigin, and M. S. Yakymenko, Phys. Lett. A **373**, 3701 (2009).
[30] Z. Zhang, C. Zhao, L. Ju, and D. G. Blair, Phys. Rev. A **81**, 013822 (2010).
[31] M. Evans, L. Barsotti, and P. Fritschel, Phys. Lett. A **374**, 665 (2010).
[32] S. E. Strigin and S. P. Vyatchanin, Phys. Lett. A **374**, 1101 (2010).
[33] S. E. Strigin, Opt. Spectrosc. **109**, 54 (2010).
[34] F. Liang, C. Zhao, S. Gras, L. Ju, and D. G. Blair, J. Phys. Conf. Ser. **228**, 012025 (2010).
[35] S. Gras, C. Zhao, D. G. Blair, and L. Ju, Class. Quantum Grav. **27**, 205019 (2010).
[36] S. E. Strigin and S. P. Vyatchanin, Gravitation Cosmol. **17**, 87 (2011).
[37] D. Heinert and S. E. Strigin, Phys. Lett. A **375**, 3804 (2011).
[38] S. E. Strigin, Opt. Spectrosc. **112**, 373 (2012).
[39] S. P. Vyatchanin and S. E. Strigin, Phys. Usp. **55**, 1115 (2012).
[40] S. L. Danilishin, S. P. Vyatchanin, D. G. Blair, J. Li, and C. Zhao, Phys. Rev. D **90**, 122008 (2014).
[41] X. Chen, C. Zhao, S. Danilishin, L. Ju, D. Blair, H. Wang, S. P. Vyatchanin, C. Molinelli, A. Kuhn, S. Gras, T. Briant, P.-F. Cohadon, A. Heidmann, I. Roch-Jeune, R. Flaminio, C. Michel, and L. Pinard, Phys. Rev. A **91**, 033832 (2015).
[42] LIGO Laboratory "LIGO web site, http://www.ligo.caltech.edu/" living document.
[43] J. Degallaix, C. Zhao, L. Ju, and D. Blair, J. Opt. Soc. Am. B **24**, 1336 (2007).
[44] L. Ju, D. G. Blair, C. Zhao, S. Gras, Z. Zhang, P. Barriga, H. Miao, Y. Fan, and L. Merrill, Class. Quantum Grav. **26**, 015002 (2009).
[45] S. Gras, D. G. Blair, and L. Ju, Phys. Lett. A **372**, 1348 (2008).
[46] S. Gras, D. G. Blair, and C. Zhao, Class. Quantum Grav. **26**, 135012 (2009).
[47] Y. Fan, L. Merrill, C. Zhao, L. Ju, D. Blair, B. Slagmolen, D. Hosken, A. Brooks, P. Veitch, and J. Munch, Class. Quantum Grav. **27**, 084028 (2010).
[48] J. Miller, M. Evans, L. Barsotti, P. Fritschel, M. MacInnis, R. Mittleman, B. Shapiro, J. Soto, and C. Torrie, Phys. Lett. A **375**, 788 (2011).
[49] C. Zhao, L. Ju, Q. Fang, C. Blair, J. Qin, D. Blair, J. Degallaix, and H. Yamamoto, arXiv:1501.01542.
[50] S. Gras, C. Zhao, L. Ju, and D. G. Blair, J. Phys. Conf. Ser. **32**, 251 (2006).
[51] Equation (9) in [31] is missing a factor of 2, resulting from a similar error in Eq. (24). This unfortunately matches a factor of 2 error in the equation for T in section 2 of [11], which should read $T = 4\pi L/(\lambda_0 Q_{\rm opt})$, such that $\delta_1 = (c/2L)(2/T)$. Note that in [31] $G_n = 2/T$ for Braginsky's Fabry-Perot cavity on resonance (i.e., with $\Delta\omega_n = 0$).
[52] LIGO Scientific Collaboration, Class. Quantum Grav. **32**, 074001 (2015).
[53] S. Gras, P. Fritschel, L. Barsotti, and M. Evans, arXiv:1502.06056.
[54] LIGO Scientific Collaboration and Virgo Collaboration, arXiv:1304.0670.